# Accepted Manuscript

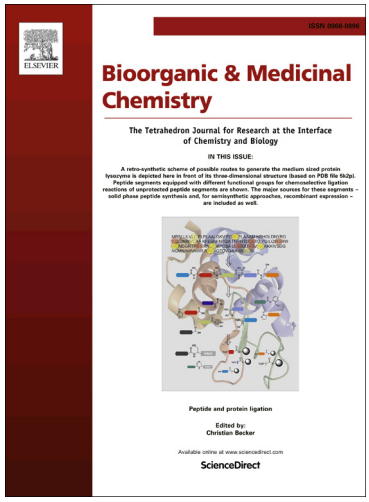


Synthesis and biological evaluation of novel synthetic chalcone derivatives as anti-tumor agents targeting Cat L and Cat K

Yali Wang, Situ Xue, Ruolan Li, Zhihui Zheng, Hong Yi, Zhuorong Li

PII: S0968-0896(17)31234-8
DOI: http://dx.doi.org/10.1016/j.bmc.2017.09.019
Reference: BMC 13979

To appear in: *Bioorganic & Medicinal Chemistry*

Received Date: 14 June 2017
Revised Date: 10 September 2017
Accepted Date: 14 September 2017

Please cite this article as: Wang, Y., Xue, S., Li, R., Zheng, Z., Yi, H., Li, Z., Synthesis and biological evaluation of novel synthetic chalcone derivatives as anti-tumor agents targeting Cat L and Cat K, *Bioorganic & Medicinal Chemistry* (2017), doi: http://dx.doi.org/10.1016/j.bmc.2017.09.019

# Synthesis and biological evaluation of novel synthetic chalcone derivatives as anti-tumor agents targeting Cat L and Cat K

Yali Wang,[a] Situ Xue,[a] Ruolan Li,[b] Zhihui Zheng,[b] Hong Yi[a] and Zhuorong Li*[a]

[a] Institute of Medicinal Biotechnology, Chinese Academy of Medical Science and Peking Union Medical College, Beijing 100050, China.

[b] New Drug Research & Development Center, North China Pharmaceutical Group Corporation, Shijiazhuang 050015, China.

## Abstract

A series of chalcone derivatives bearing benzamide or benzenesulfonamide moieties were synthesized and evaluated for their anti-tumor effect on HCT116, MCF7 and 143B cell lines *in vitro*. SAR analysis showed that compounds bearing a benzenesulfonamide group had greater potency than those bearing a benzamide group. It was also shown that compounds with a mono-methyl or mono-halogen group at the 3-position on the terminal phenyl ring were more effective than those with trifluoromethyl or methoxy groups. Compound **8e** exhibited the most potent anti-tumor activities against HCT116, MCF7 and 143B cell lines, with $IC_{50}$ values of 0.597, 0.886 and 0.791 μM, respectively. Molecular docking studies and enzymatic assays demonstrated that the anti-tumor activity of compound **8e** might be regulated by Cat L and Cat K.

**Key words:** Anti-tumor activity, chalcone, Cat L, Cat K

## 1. Introduction

Cathepsins, which are involved in numerous physiological processes, can be divided into three subgroups based on their active site amino acid; namely, cysteine (B, C, F, H, K, L, O, S, V, W and X), aspartic (D and E), and serine (G) cathepsins.[1] Cysteine cathepsins have been reported to be important in a variety of physiological and pathological processes, such as tumor progression and metastasis,[2-5] osteoporosis,[6] osteoarthritis[7] and atherosclerosis.[8] There is now good evidence that several cysteine cathepsins, including cathepsin (Cat) B, F, H, L, K, S, V and X, are related to the progression of cancer.[5] Increased expression of cysteine cathepsins has been shown to correlate with malignancy and poor prognosis of patients, indicating their potential diagnostic and prognostic value.[9, 10]

The upregulation of Cat L has been reported in a wide range of human malignancies including colon,[11] breast,[12] lung,[13] melanoma[14] and pancreatic[15] cancers. Cat L is required for cell cycle progression and knockout models exhibit reduced cell proliferation and tumor growth.[1] Cat K is overexpressed in melanoma,[16] prostate cancer,[17] giant cell tumors[18] and basal cell carcinoma,[19] and has also been implicated

* Corrseponding anthor: e-mail: lizhuorong@imb.pumc.edu.cn; Tel: +86-10-83152017.

in breast cancer[20] and osteosarcoma.[21] Odanacatib, a Cat K inhibitor, has been shown to have good therapeutic effects in patients with breast cancer.[22] The fact that a cysteine cathepsin inhibitor can reduce tumor growth, invasion and metastasis suggests that targeting cysteine cathepsins could be therapeutically beneficial.[23, 24]

To date, there have been lots of compounds explored as cysteine cathepsin inhibitors and the representative structure were presented in Figure 1. Several other compounds such as quinazoline,[25] chalone,[26-29] pyrazoline,[30] semicarbazone[30] and thiosemicarbazone,[31] also have activity against cathepsins. Chalcones are an important type of natural product and exhibit a wide range of biological effects,[32] including acting as anticancer, anti-inflammatory, antiviral and antimicrobial agents. Ramalho *et al.* reported on a series of chalcones that showed cytotoxic activity along with Cat K inhibition.[28] Cyclohexenyl chalcones panduratin A and nicolaioidesin C demonstrate a high level of cytotoxicity in various human cancer cells through inhibiting the Cat L enzyme.[33] These examples highlight the growing interest in new chalcone derivatives as cysteine cathepsin inhibitors, which prompted us to further investigate this drug skeleton.

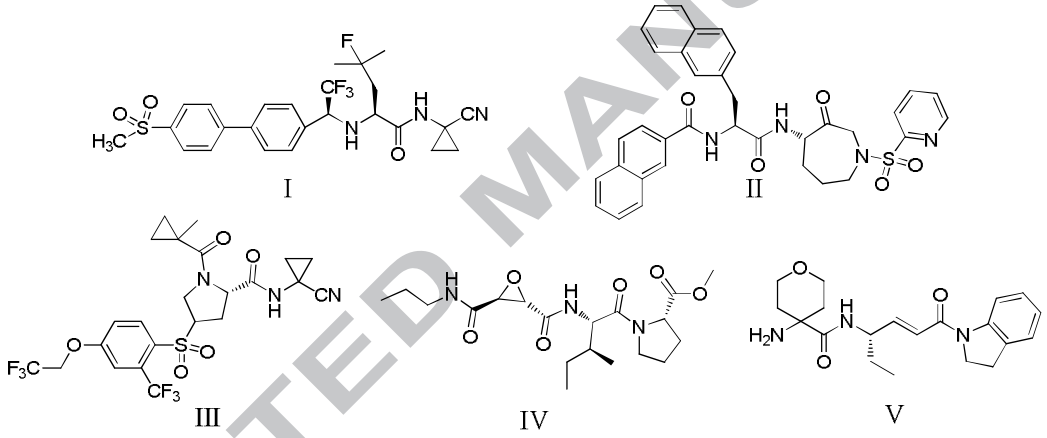


**Figure 1.** Representative inhibitors of cysteine cathepsins, including Cat K (I),[34] Cat L (II),[31] Cat S (III),[35] Cat B (IV)[36] and Cat C (V)[37].

Cysteine residues are known to be key amino acids in the active site of cysteine cathepsins, where the reactive electrophilic warhead could interact with the thiol moiety of cysteine.[38] The electrophilic carbonyl, sulfonyl and nitrile groups act as warheads in mediating covalent reversible inhibition. In the present study, benzamide or benzenesulfonamide groups with carbonyl or sulfonyl pharmacophores were introduced to the chalcone skeleton, which resulted in promising anti-cysteine cathepsin activity. We also introduced an imidazole group to the chalcone skeleton to enhance the anti-cancer activity, as in reported studies.[39]

All target compounds were evaluated for their *in vitro* cytotoxicity against HCT116 (human colon cancer), MCF7 (human breast cancer) and 143B (human osteosarcoma) cell lines. Compounds possessing the greatest apparent cytotoxic activity were evaluated for their ability to inhibit specific enzymes *in vitro*. Lastly, *in silico* molecular docking of the most promising compound **8e** were carried out.

## 2. Chemistry

The synthesis of target compounds **6a**–**o** is illustrated in Scheme 1. The commercially available 1,2-diaminobenzene and 2-hydroxypropanoic acid were refluxed in 4N aqueous HCl solution to afford **1**,[40] which was precipitated from the reaction mixture after neutralization with aqueous $NH_3$ solution. Treatment of **1** with 2,2,6,6-tetramethylpiperidin (TEMPO), sodium hypochlorite and potassium bromide at 10–15°C afforded intermediate **2**. The aldehyde group of 3-nitrobenzaldehyde was protected by ethylene in toluene at 120 °C to obtain **3**.[41] The reduction of **3** with hydrogen and catalytic amounts of Pd/C in methanol yielded **4** at room temperature.[42] Next, **4** was acylated with corresponding benzoyl chloride in the presence of pyridine in dichloromethane, with further treatment in aqueous HCl solution mixed with 1,4-dioxane at 50°C to obtain **5a**–**o**. Finally, target compounds **6a**–**o** were successfully obtained via the condensation of **5a**–**o** with intermediate **2** in ethanol. The synthesis of target compounds **8a**–**i** is shown in Scheme 2. Following the procedure for **5a**–**o**, the intermediates **7a**–**i** were obtained from intermediate **4** with benzene sulfonyl chloride. Target compounds **8a**–**i** were obtained using the same methods as for **6a**–**o**.

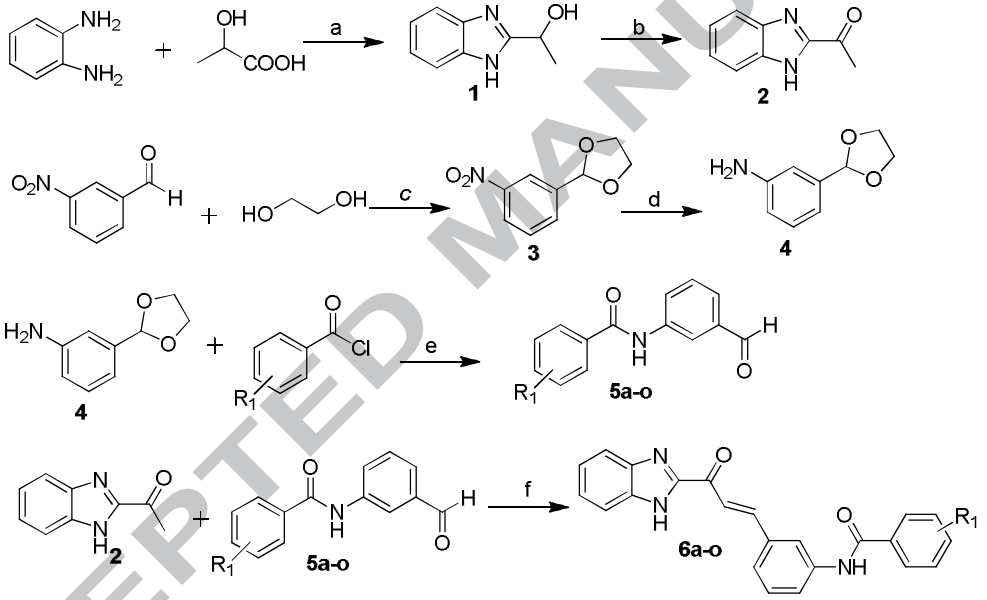


**Scheme 1.** Synthetic route for target compounds **6a**–**o**. Reagents and conditions: (a) 4N HCl, reflux, 5 h; (b) TEMPO, NaClO, KBr, $CH_3CN$, 10–15 °C; (c) *p*-TsOH, toluene, reflux, 8 h; (d) Pd/C, $H_2$, $CH_3OH$, rt; (e) (i) Py, $CH_2Cl_2$, rt; (ii) HCl, 1,4-dioxane, 50 °C; (f) NaOH, $C_2H_5OH$.

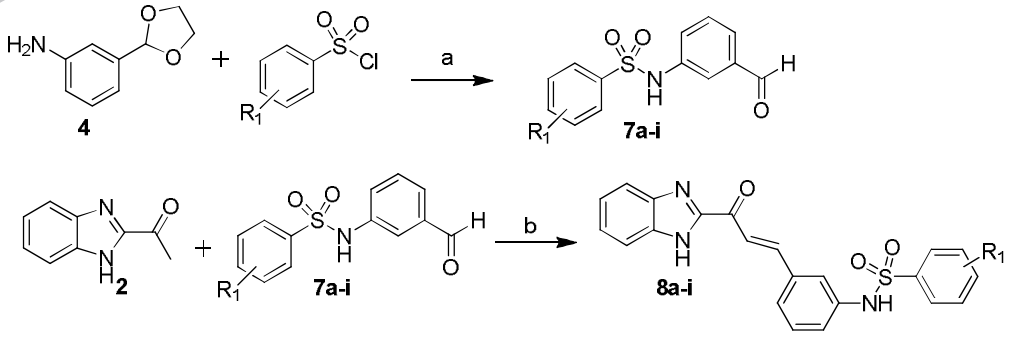

**Scheme 2.** Synthetic route for target compounds **8a**–**i**. Reagents and conditions: (a) (i) Py, $CH_2Cl_2$, rt; (ii) HCl, 1,4-dioxane, 50 °C; (b) NaOH, $C_2H_5OH$.

## 3. Results and Discussion

*3.1. In vitro anti-tumor activities and structure-activity relationships*

The anti-tumor activities of the target compounds were evaluated against HCT116, MCF7 and 143B cell lines using the MTT assay. The bioactivity data was summarized in Tables 1 and 2, using 5-FU, paclitaxel and odanacatib as the positive controls.

**Table 1** The anti-tumor activities of **6a**–**o** against HCT116, MCF7 and 143B cell lines *in vitro*

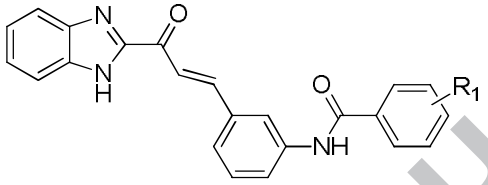


| Compd. | $R_1$ | $IC_{50}$ (μM) ± SD | | |
|---|---|---|---|---|
| | | HCT116 | MCF7 | 143B |
| **6a** | H | 2.443 ± 0.422 | 11.232 ± 1.492 | 8.340 ± 1.244 |
| **6b** | 2-Cl | 1.282 ± 0.059 | 4.568 ± 0.030 | 3.692 ± 0.699 |
| **6c** | 3-Cl | 1.123 ± 0.154 | 7.835 ± 1.588 | 3.370 ± 0.188 |
| **6d** | 4-Cl | 2.267 ± 0.138 | 8.409 ± 0.672 | 7.441 ± 0.632 |
| **6e** | 2-Br | 1.680 ± 0.091 | 4.519 ± 0.443 | 6.047 ± 0.105 |
| **6f** | 3-Br | 1.555 ± 0.251 | 5.209 ± 0.100 | 4.624 ± 0.220 |
| **6g** | 4-Br | 2.225 ± 0.890 | 7.002 ± 13.102 | 7.314 ± 0.173 |
| **6h** | 2-$CH_3$ | 1.869 ± 1.616 | 5.867 ± 0.114 | 8.285 ± 0.117 |
| **6i** | 3-$CH_3$ | 1.418 ± 0.260 | 5.594 ± 0.746 | 4.882 ± 0.847 |
| **6j** | 4-$CH_3$ | 1.662 ± 0.338 | 9.692 ± 0.613 | 6.564 ± 1.271 |
| **6k** | 3-$CF_3$ | 3.362 ± 0.162 | 21.470 ± 7.655 | 9.570 ± 0.452 |
| **6l** | 3-$OCH_3$ | 3.681 ± 0.236 | 17.840 ± 0.175 | 4.607 ± 0.423 |
| **6m** | 4-$OCH_3$ | 4.882 ± 0.954 | 20.134 ± 1.025 | 6.328 ± 0.502 |
| **6n** | 3,5-$(Cl)_2$ | 1.645 ± 0.352 | > 100 | 3.657 ± 0.242 |
| **6o** | 3,5-$(CH_3)_2$ | 1.553 ± 0.148 | 24.608 ± 6.951 | 4.015 ± 0.631 |
| **5-FU** | - | 8.638 ± 1.639 | 32.626 ± 2.785 | 25.216 ± 1.058 |
| **Paclitaxel** | - | 0.014 ± 0.005 | 1.428 ± 0.389 | 5.560 ± 0.495 |
| **Odanacatib** | - | > 100 | 45.379 ± 3.094 | 12.715 ± 1.411 |

As illustrated in Tables 1 and 2, most of the target compounds **6a**–**o** and **8a**–**i** were shown to have anti-tumor activities. With the exception of **6n**, all other compounds demonstrated greater potency than 5-FU, and all of the compounds showed greater potency than odanacatib. Some compounds were more potent than paclitaxel against one or more of the tumor cell lines. Compound **6a**, which lacked a substituent ($R_1$ = H) on the terminal phenyl ring, showed moderate activity against HCT116, MCF7 and 143B cell lines, with $IC_{50}$ values of 2.443, 11.232 and 8.340 μM, respectively. The introduction of a mono-halogen (**6b**–**g**, $R_1$ = 2-Cl, 3-Cl, 4-Cl, 2-Br, 3-Br and 4-Br,

respectively) led to an improvement in activities compared to **6a**. Compounds **6h–j** with mono-methyl groups ($R_1$ = 2-$CH_3$, 3-$CH_3$, and 4-$CH_3$, respectively) also showed greater activity than **6a**. However, the introduction of a double chlorine or double methyl group (**6n**, $R_1$ = 3,5-$(Cl)_2$; **6o**, $R_1$ = 3,5-$(CH_3)_2$) resulted in lower potency than mono-substitution (**6c** and **6i**). Compound **6k** with a 3-$CF_3$ substitution had lower activity than **6a**. The introduction of a methoxy group (**6l**, $R_1$ = 3-$OCH_3$; **6m**, $R_1$ = 4-$OCH_3$) led to higher activity against the 143B cell line, but lower activity against HCT116 and MCF7 cell lines, compared to **6a**. Interestingly, the position of the $R_1$ group was closely related to the anti-tumor activity. Compounds with a 3-substituted phenyl group (**6c**, **6f** and **6i**) exhibited higher potency than those with a 2-substituted (**6b**, **6e** and **6h**) or 4-substituted phenyl group (**6d**, **6g** and **6j**). Another interesting phenomenon observed was that when introducing a group with strong electron-withdrawing ability (**6k**, $R_1$ = 3-$CF_3$) or electron-donating ability (**6l**, $R_1$ = 3-$OCH_3$) into the 3-position, the resulting activity was lower than that of **6a**. However, the introduction of a chlorine (**6c**, $R_1$ = 3-Cl) or methyl (**6i**, $R_1$ = 3-$CH_3$) group into the 3-position resulted in higher potency than **6a**. We therefore predicted that a suitable electron density within the terminal phenyl would be favorable to drug activity.

Preliminary structure-activity relationships (SARs) for compounds **8a-i** were also analyzed. Similar to the SARs for **6a–o**, compounds with a 3-substituted phenyl group (**8b** and **8e**) showed higher potency than those with a 2-substituted (**8a** and **8d**) or 4-substituted phenyl group (**8c** and **8f**). The introduction of double chlorine or methyl groups (**8g** and **8i**) led to reduced activity compared to the mono-substituent (**8b** and **8d**).

**Table 2** The anti-tumor activities of **8a-i** against HCT116, MCF7 and 143B cell lines *in vitro*

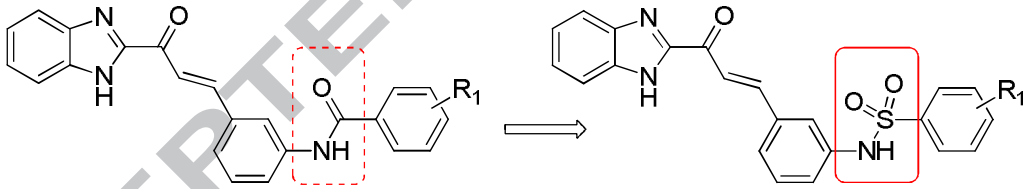

| Compd. | $R_1$ | $IC_{50}$ (μM) ± SD | | |
|---|---|---|---|---|
| | | HCT116 | MCF7 | 143B |
| **8a** | 2-Cl | 0.987 ± 0.034 | 4.284 ± 0.653 | 4.789 ± 0.140 |
| **8b** | 3-Cl | 0.737 ± 0.068 | 4.159 ± 0.113 | 2.506 ± 0.055 |
| **8c** | 4-Cl | 1.956 ± 0.255 | 3.822 ± 0.573 | 7.445 ± 2.198 |
| **8d** | 2-$CH_3$ | 0.955 ± 0.153 | 4.132 ± 0.204 | 4.063 ± 0.617 |
| **8e** | 3-$CH_3$ | 0.597 ± 0.166 | 0.886 ± 0.131 | 0.791 ± 0.078 |
| **8f** | 4-$CH_3$ | 1.989 ± 0.126 | 3.216 ± 0.108 | 3.220 ± 0.243 |
| **8g** | 3,5-$(Cl)_2$ | 2.844 ± 1.038 | 19.995 ± 6.169 | 5.951 ± 0.162 |
| **8h** | 3,4-$(CH_3)_2$ | 1.224 ± 0.294 | 4.566 ± 0.297 | 3.330 ± 0.927 |
| **8i** | 3,5-$(CH_3)_2$ | 2.230 ± 1.451 | 5.859 ± 1.084 | 5.048 ± 0.035 |
| **5-FU** | - | 8.638 ± 1.639 | 32.626 ± 2.785 | 25.216 ± 1.058 |
| **Paclitaxel** | - | 0.014 ± 0.005 | 1.428 ± 0.389 | 5.560 ± 0.495 |
| **Odanacatib** | - | > 100 | 45.379 ± 3.094 | 12.715 ± 1.411 |

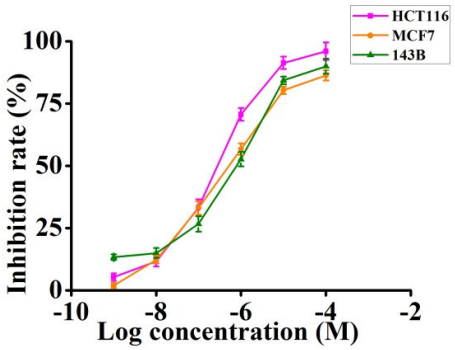


**Figure 2.** Inhibitory curves of compound **8e** toward HCT116 (magenta), MCF7 (orange) and 143B (olive) cell lines.

In general, the data listed in Tables 1 and 2 showed that the activity of compounds **8a**–**i** was higher than that of compounds **6a**–**o**, demonstrating that introducing a benzenesulfonamide group led to greater potency than introducing a benzamide group. Compound **8e** showed the most potent anti-tumor activity against HCT116, MCF7 and 143B cell lines, with $IC_{50}$ values of 0.597, 0.886 and 0.791 μM, respectively. The inhibitory curves (Figure 2) showed that the effects of **8e** were dose-dependent.

*3.2. In silico molecular docking studies and in vitro enzymatic assays*

To investigate the biological mechanisms of action, molecular docking studies combined with *in vitro* enzymatic assays were implemented. The crystal structures of eight cancer-associated cysteine cathepsins were processed using the protein preparation protocol of Sybyl-X2.0 (Tripos, USA) and the location of the ligand in the co-crystal structure was defined as the active site. Compound **8e** was docked into the active sites of eight crystal structures, respectively. A high absolute docking score demonstrated possible enzymatic activity. According to the results shown in Table 4, Cat B, Cat L, Cat K and Cat S exhibited the best docking scores (< −7 kcal/mol). These four enzymes were selected to investigate further.

**Table 4** Docking scores of compound **8e** with eight cancer-associated cysteine cathepsins.

| Enzyme/Pdb Code | Docking score (kcal.mol$^{-1}$) |
|---|---|
| Cat B/1GMY | -7.46 |
| Cat F/1M6D | -5.75 |
| Cat H/1NB3 | -5.14 |
| Cat L/4AMX | -7.83 |
| Cat K/1NLJ | -7.96 |
| Cat S/4BS5 | -7.70 |
| Cat V/1FHO | -6.14 |
| Cat X/1EF7 | -5.93 |

Eight compounds were screened against Cat L, Cat K, Cat B and Cat S at 5 μM. The results summarized in Table 5 are expressed as inhibition rates (%). Against Cat L,

compounds **8e** and **8f** showed > 90% inhibition; compounds **6c** and **6i** showed 80–90% inhibition; and compounds **8b** and **8d** showed 70–80% inhibition. Most of the tested compounds demonstrated greater potency than odanacatib. Against Cat K, compounds **8d** and **8e** showed > 90% inhibition; compounds **8a**, **8b** and **8f** showed 80–90% inhibition; and compounds **6c** and **6i** showed 70–80% inhibition. In short, most of them showed superior activity against Cat K. Against Cat B, all compounds resulted in lower than 50% inhibition. Against Cat S, compound **8c** showed 89.35% inhibition, while all other compounds showed lower enzymatic activity. The enzyme activity of these compounds was obviously improved compared with the compound without benzenesulfonamide or benzamide group (Table S1). In general, these compounds showed dual activity against Cat K and Cat L, whereas the effects on Cat B and Cat S were weaker. Importantly, compound **8e**, which showed > 90% inhibition of Cat L and Cat K, also exhibited the best anti-tumor activity against HCT116, MCF7 and 143B cell lines. We speculated that compound **8e** exhibited anti-tumor activity through targeting Cat L and Cat K. Further research into the mechanisms of these compounds was required.

**Table 5** The inhibitory rate of Cat L, Cat K, Cat B and Cat S by target compounds

| Compd. | Enzyme Inhibition (5 μM, %) | | | |
|---|---|---|---|---|
| | Cat L | Cat K | Cat B | Cat S |
| **6c** | 86.00 ± 14.16 | 72.99 ± 5.12 | 30.49 ± 4.43 | 19.47 ± 3.17 |
| **6i** | 88.54 ± 12.49 | 77.97 ± 7.34 | 41.30 ± 7.29 | 45.17 ± 3.55 |
| **8a** | 62.94 ± 5.32 | 86.48 ± 5.95 | 32.48 ± 5.22 | 45.73 ± 7.27 |
| **8b** | 78.88 ± 7.44 | 89.15 ± 6.76 | 15.24 ± 3.89 | 52.61 ± 4.96 |
| **8c** | 57.99 ± 10.30 | 58.14 ± 5.33 | 23.75 ± 4.11 | 89.35 ± 5.53 |
| **8d** | 71.28 ± 6.32 | 91.27 ± 7.12 | 40.02 ± 5.28 | 47.75 ± 5.19 |
| **8e** | 92.35 ± 8.87 | 93.46 ± 7.88 | 45.63 ± 4.99 | 50.13 ± 4.20 |
| **8f** | 93.79 ± 12.53 | 85.96 ± 6.53 | 34.26 ± 7.21 | 21.97 ± 4.37 |
| **Odanacatib** | 71.28 ± 11.25 | 100 ± 0 | 100 ± 0 | 100 ± 0 |
| **E64** | 100 ± 0 | 100 ± 0 | 100 ± 0 | 100 ± 0 |
| **CA074** | - | - | 100 ± 0 | - |

*3.3. In silico docking analysis*

In order to observe the possible binding modes of compound **8e** in the Cat L and Cat K active sites, *in silico* docking results were analyzed. The proposed binding mode of compound **8e** in the Cat L active site is shown in Figure 3(A). In this model, one oxygen atom from the sulfonyl group serves as an acceptor to form H-bonds with Cys25 and His164; the amino of the sulfamide group donates one H-bond to Gly68; and the oxygen atom of the carbonyl group serves as an acceptor to form H-bonds with Gln19 and His163. A suggested binding model for compound **8e** in the Cat K active site is shown in Figure 3(B). In this model, two oxygen atoms from the sulfonyl group serve as acceptors to form H-bonds with Cys25, His162, Gln19 and Trp184; and the amino of the imidazole ring serves as a donor to form an H-bond with Gly64.

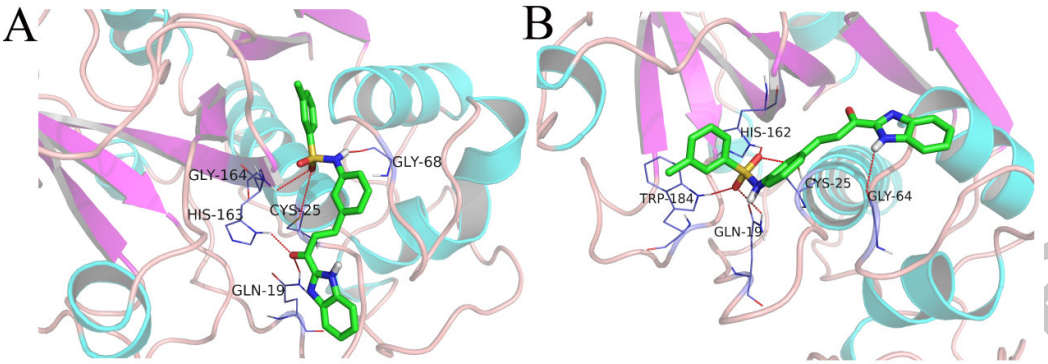


**Figure 3.** (A) The virtual binding mode of compound **8e** in the Cat L active site. (B) The virtual binding mode of compound **8e** in the Cat K active site. Compound **8e** is represented as stick diagrams with carbon atoms shown in green. Relevant amino acid residues in the binding site are shown in line. Red dashed lines represent H-bonds. Pictures were generated using Pymol.

From the docking results exhibited in Figure 3, we concluded that the binding modes of compound **8e** were different in the Cat L and Cat K active sites. Whereas, **8e** could form an H-bond interaction with Cys25, which is a crucial amino acid residue in both of the Cat L and Cat K active sites. The sulfonyl group of **8e** appears to act as a reactive electrophilic warhead that interacts with the thiol moiety of Cys25. Furthermore, the carbonyl group introduced to the compound (6i) could also form an H-bond interaction with Cys25 (Figure S1).

## 4. Conclusions

In this study, a library of new chalcone analogs possessing benzamide or benzenesulfonamide scaffolds were synthesized and evaluated for their biological activity. Preliminary investigation indicated that the series containing benzenesulfonamide scaffolds demonstrate higher levels of anti-tumor activity than those based on a benzamide scaffold. The most promising compound, **8e**, had $IC_{50}$ values of 0.597, 0.886 and 0.791 μM against HCT116, MCF7 and 143B cell lines, respectively. A SAR study showed that substituting either a mono-methyl or mono-halogen group at the 3-position on the terminal phenyl ring was beneficial in terms of anti-tumor activity. Docking studies demonstrated that compound **8e** formed H-bond interactions with Gln19, Cys25, Gly68, His163 and Gly164 in the Cat L active site, and Gln19, Cys25, Gly64, His162 and Trp184 in the Cat K active site. Enzymatic assays revealed that **8e** (5 μM) inhibited Cat L and Cat K by 92.35% and 93.46%, respectively. Combined results from enzymatic assays and molecular docking analysis therefore indicated that Cat L and Cat K might be potential targets for compound **8e**.

## 5. Experimental section

*5.1. General procedures*

All melting points (m.p.) were determined using an MP90 automated melting point

instrument (Mettler Toledo, Switzerland) and were uncorrected. Mass spectra (MS) and high resolution mass spectra (HRMS) were performed using an LCMS-2020 (Shimadzu, Japan) and an LTQ Orbitrap XL (Thermo Scientific, USA), respectively. $^{1}H$ and $^{13}C$ NMR spectra were performed using a Bruker BioSpin GmbH spectrometer (Bruker Bioscience, USA). Column chromatography was performed using a 200–300 mesh silica gel from Qingdao Ocean Chemical. Unless specified, all reagents were obtained from commercially available sources and were used without purification.

*5.2. Chemical synthesis*

*1-(1H-benzo[d]imidazol-2-yl) ethanol (**1**)*

A mixture of 1,2-diaminobenzene (5.41 g, 0.05 mol), 2-hydroxypropanoic acid (7.95 g, 85% in water, 0.075 mol) and 4 N aqueous HCl solution (40 mL) was refluxed for 5 h. After cooling to room temperature, the reaction mixture was neutralized with aqueous $NH_3$ solution. The precipitant was then filtered, washed with water and dried to afford compound **1**, a grey-white solid with 80% yield, MS (ESI) m/z: 163 $(M+H)^+$. The $^{1}H$ NMR spectrum was in accordance with that described in the literature.[40]

*1-(1H-benzo[d]imidazol-2-yl) ethanone (**2**)*

To a solution of **1** (1.62 g, 0.01 mol), 2,2,6,6-tetramethylpiperidin (0.016 g, 0.1 mmol) and potassium bromide (0.12 g, 1 mmol) in 40 mL acetonitrile/water (1:1), 8% aqueous sodium hypochlorite (13.96 g, 0.015 mol) was added over a 15–20 minute period, keeping the temperature of the reaction mixture between 10 and 15°C. The mixture was stirred for 30 minutes and was extracted with ethyl acetate (50 mL × 3). The combined extracts were washed with 60 mL of 10% aqueous sodium thiosulfate and 60 mL of saturated sodium chloride solution. The organic phase was separated, dried over anhydrous $MgSO_4$ and evaporated to afford compound **2** with 85% yield, MS (ESI) m/z: 161 $(M+ H)^+$. $^{1}H$ NMR (400 MHz, DMSO) δ 13.31 (s, 1H), 7.84 (d, $J$ = 8.1 Hz, 1H), 7.57 (d, $J$ = 8.1 Hz, 1H), 7.39 (t, $J$ = 7.1 Hz, 1H), 7.31 (d, $J$ = 7.2 Hz, 1H), 2.72 (s, 3H).

*2-(3-Nitro-phenyl)-1,3-dioxolane (**3**)*

A solution of 3-nitrobenzaldehyde (4.53 g, 0.03 mol), ethylene glycol (2.05 g, 0.033 mol) and *p*-toluenesulfonic (0.02 g, 0.1 mmol) in 150 mL toluene was refluxed under a Dean-Stark trap for 10 h. The reaction mixture was then cooled to room temperature and washed with saturated sodium bicarbonate solution and saturated sodium chloride solution, and dried with anhydrous $MgSO_4$. Evaporation of the organic phase gave compound **3** with 95% yield. The $^{1}H$ NMR spectrum was in accordance with that described in the literature.[41]

*3-(1,3-Dioxolan-2-yl)aniline (**4**)*

A mixture of compound **3** (1.95 g, 0.01 mol) and Pd/C (0.1 g, 10%) in 50 mL methanol was stirred under hydrogen at room temperature for 4 h. The reaction mixture was filtered and the filtrate was evaporated to afford compound **4**, a yellow oil with 97% yield, MS (ESI) m/z: 166 $(M+ H)^+$. The $^{1}H$ NMR spectrum was in

accordance with that described in the literature.[42]

*General procedure for preparation of intermediates (**5a–o**)*

To a stirred solution of compound **4** (0.50 g, 3 mmol) in 15 mL dichloromethane, pyridine (0.24 mL, 3 mmol) and corresponding benzoyl chloride (3 mmol) were added at 0°C. The reaction mixture was stirred for 30 minutes, after which it was washed with 10 mL 4N aqueous HCl solution and 10 mL saturated sodium chloride solution. The organic layer was dried with anhydrous $MgSO_4$ and concentrated. The residue was dissolved in 20 mL dioxane and then 15 mL of a 4N aqueous HCl solution was added at room temperature. The reaction mixture was stirred at 50°C for 30 minutes after which it was extracted with ethyl acetate (50 mL × 3). The extract was washed with saturated sodium chloride solution and dried with anhydrous $MgSO_4$. After concentration, column chromatography of the residue on silica gel (eluent PE/EA 7:1) generated compounds **5a**–**o**. The spectral data are summarized in the Supplementary Information.

*General procedure for preparation of target compounds (**6a–o**)*

A mixture of an appropriate *intermediates* **5a**–**o** (3 mmol), compound **2** (0.48 g, 3 mmol) and sodium hydroxide (0.12 g, 3 mmol) in ethanol (15 mL) was stirred at room temperature for 24 h. Distilled water (5 mL) was added and the precipitate was collected by filtration. Subsequently, it was purified by recrystallization with methanol to afford the target compounds **6a**–**o**.

*(E)-N-(3-(3-(1H-benzo[d]imidazol-2-yl)-3-oxoprop-1-en-1-yl)phenyl)benzamide (**6a**).* Yellow solid; yield: 53%; m.p.: 233.5–235.2 °C; $^1$H NMR (400 MHz, DMSO) δ 10.45 (s, 1H), 8.39 (s, 1H), 8.15 (d, *J* = 16.1 Hz, 1H), 8.04–7.96 (m, 4H), 7.80–7.65 (m, 2H), 7.64–7.61 (m, 1H), 7.56 (m, 3H), 7.49 (t, *J* = 7.8 Hz, 1H), 7.39 (s, 2H); $^{13}$C NMR (101 MHz, DMSO) δ 181.25, 166.21, 149.47, 144.50, 140.42, 135.17, 132.23, 130.03, 128.92, 128.17, 126.09, 123.41, 122.00, 119.14; HRMS calcd for $C_{23}H_{18}N_3O_2$ $(M+H)^+$ 368.13935, found 368.13921.

*(E)-N-(3-(3-(1H-benzo[d]imidazol-2-yl)-3-oxoprop-1-en-1-yl)phenyl)-2-chlorobenza mide (**6b**).* Yellow solid; yield: 54%; m.p.: 275.5–277.3 °C; $^1$H NMR (400 MHz, DMSO) δ 10.72 (s, 1H), 8.33 (s, 1H), 8.13 (d, *J* = 16.1 Hz, 1H), 7.96 (d, *J* = 16.1 Hz, 1H), 7.87 (t, *J* = 8.3 Hz, 2H), 7.65 (dd, *J* = 7.2, 1.1 Hz, 1H), 7.60 (d, *J* = 7.8 Hz, 3H), 7.56–7.48 (m, 3H), 7.41 (t, *J* = 7.5 Hz, 1H), 7.33 (t, *J* = 7.5 Hz, 1H); $^{13}$C NMR (101 MHz, DMSO) δ 181.20, 165.65, 149.42, 144.29, 143.51, 140.11, 137.18, 135.30, 135.25, 131.69, 130.41, 130.21, 130.15, 129.44, 127.74, 126.28, 126.03, 123.66, 122.66, 122.13, 121.64, 118.50, 113.36; HRMS calcd for $C_{23}H_{17}ClN_3O_2$ $(M+H)^+$ 402.10038, found 402.10029.

*(E)-N-(3-(3-(1H-benzo[d]imidazol-2-yl)-3-oxoprop-1-en-1-yl)phenyl)-3-chlorobenza mide (**6c**).* Yellow solid; yield: 57%; m.p.: 205.5–206.9 °C; $^1$H NMR (400 MHz, DMSO) δ 10.53 (s, 1H), 8.36 (s, 1H), 8.14 (d, *J* = 16.1 Hz, 1H), 8.07 (s, 1H),

7.99–7.95 (m, 3H), 7.75 (s, 2H), 7.69 (d, *J* = 7.9 Hz, 1H), 7.62–7.57 (m, 2H), 7.49 (t, *J* = 7.8 Hz, 1H), 7.38 (dd, *J* = 6.0, 3.1 Hz, 2H); $^{13}$C NMR (101 MHz, DMSO) δ 181.16, 164.68, 149.39, 144.40, 140.10, 137.09, 135.11, 133.73, 132.02, 130.89, 130.04, 127.91, 126.98, 126.27, 123.44, 122.04, 119.24; HRMS calcd for $C_{23}H_{17}ClN_3O_2$ $(M+H)^+$ 402.10038, found 402.10037.

*(E)-N-(3-(3-(1H-benzo[d]imidazol-2-yl)-3-oxoprop-1-en-1-yl)phenyl)-4-chlorobenzamide (**6d**).* Yellow solid; yield: 62%; m.p.: 250.1–252.9 °C; $^1$H NMR (400 MHz, DMSO) δ 10.50 (s, 1H), 8.36 (s, 1H), 8.14 (d, *J* = 16.1 Hz, 1H), 8.045 (d, *J* = 8.6 Hz, 2H), 7.99–7.95 (m, 2H), 7.75 (s, 2H), 7.64 (d, *J* = 8.5 Hz, 2H), 7.56 (d, *J* = 7.7 Hz, 1H), 7.49 (t, *J* = 7.8 Hz, 1H), 7.38 (dd, *J* = 6.2, 3.1 Hz, 2H); $^{13}$C NMR (101 MHz, DMSO) δ 181.19, 165.09, 149.42, 144.45, 140.21, 137.09, 135.12, 133.84, 130.13, 129.00, 126.20, 123.45, 122.03, 119.24; HRMS calcd for $C_{23}H_{17}ClN_3O_2$ $(M+H)^+$ 402.10038, found 402.10038.

*(E)-N-(3-(3-(1H-benzo[d]imidazol-2-yl)-3-oxoprop-1-en-1-yl)phenyl)-2-bromobenzamide (**6e**).* Yellow solid; yield: 64%; m.p.: 276.2–278.1 °C; $^1$H NMR (400 MHz, DMSO) δ 10.70 (s, 1H), 8.33 (s, 1H), 8.13 (d, *J* = 16.1 Hz, 1H), 7.96 (d, *J* = 16.1 Hz, 1H), 7.86 (d, *J* = 8.0 Hz, 1H), 7.75 (dd, *J* = 7.9, 0.9 Hz, 3H), 7.65–7.58 (m, 2H), 7.55–7.50 (m, 2H), 7.48–7.43 (m, 1H), 7.40–7.37 (m, 2H); $^{13}$C NMR (101 MHz, DMSO) δ 181.17, 166.56, 149.40, 144.36, 140.16, 139.37, 135.26, 133.24, 131.80, 130.23, 129.38, 128.23, 126.05, 122.70, 122.14, 119.46, 118.52; HRMS calcd for $C_{23}H_{17}BrN_3O_2$ $(M+H)^+$ 446.04987, found 446.04990.

*(E)-N-(3-(3-(1H-benzo[d]imidazol-2-yl)-3-oxoprop-1-en-1-yl)phenyl)-3-bromobenzamide (**6f**).* Yellow solid; yield: 45%; m.p.: 233.2–235.1 °C; $^1$H NMR (400 MHz, DMSO) δ 10.56 (s, 1H), 8.36 (s, 1H), 8.21 (s, 1H), 8.15 (d, *J* = 16.0 Hz, 1H), 8.02 (d, *J* = 7.7 Hz, 1H), 7.96 (t, *J* = 7.9 Hz, 2H), 7.81 (d, *J* = 7.8 Hz, 1H), 7.76 (dd, *J* = 5.7, 3.0 Hz, 2H), 7.59 (d, *J* = 7.5 Hz, 1H), 7.51 (m, 2H), 7.40 (dd, *J* = 6.0, 3.0 Hz, 2H); $^{13}$C NMR (101 MHz, DMSO) δ 180.77, 164.62, 149.02, 144.68, 140.13, 137.28, 135.09, 134.94, 131.15, 130.78, 127.39, 126.18, 125.26, 123.58, 122.21, 122.02, 119.54; HRMS calcd for $C_{23}H_{17}BrN_3O_2$ $(M+H)^+$ 446.04987, found 446.04982.

*(E)-N-(3-(3-(1H-benzo[d]imidazol-2-yl)-3-oxoprop-1-en-1-yl)phenyl)-4-bromobenzamide (**6g**).* Yellow solid; yield: 60%; m.p.: 282.2–283.7 °C; $^1$H NMR (400 MHz, DMSO) δ 10.50 (s, 1H), 8.35 (s, 1H), 8.14 (d, *J* = 16.1 Hz, 1H), 7.96 (t, *J* = 7.9 Hz, 4H), 7.78 (d, *J* = 8.4 Hz, 4H), 7.56 (d, *J* = 7.6 Hz, 1H), 7.49 (t, *J* = 7.8 Hz, 1H), 7.38 (dd, *J* = 5.8, 2.8 Hz, 2H); $^{13}$C NMR (101 MHz, DMSO) δ 181.21, 165.20, 149.44, 144.42, 140.20, 135.12, 134.21, 131.94, 130.30, 130.05, 126.22, 126.04, 123.44, 122.04, 119.21; HRMS calcd for $C_{23}H_{17}BrN_3O_2$ $(M+H)^+$ 446.04987, found 446.04991.

*(E)-N-(3-(3-(1H-benzo[d]imidazol-2-yl)-3-oxoprop-1-en-1-yl)phenyl)-2-methylbenzamide (**6h**).* Yellow solid; yield: 55%; m.p.: 264.1–265.9 °C; $^1$H NMR (400 MHz,

DMSO) δ 13.53 (s, 1H), 10.49 (s, 1H), 8.36 (s, 1H), 8.12 (d, *J* = 16.1 Hz, 1H), 7.95 (d, *J* = 16.0 Hz, 1H), 7.88 (d, *J* = 8.1 Hz, 2H), 7.60 (d, *J* = 8.1 Hz, 1H), 7.57 (d, *J* = 7.7 Hz, 1H), 7.53 (d, *J* = 7.2 Hz, 1H), 7.48 (t, *J* = 7.9 Hz, 1H), 7.42 (t, *J* = 7.3 Hz, 2H), 7.53 (m, 3H), 2.44 (s, 3H); $^{13}$C NMR (101 MHz, DMSO) δ 181.25, 168.58, 149.45, 144.49, 143.52, 140.49, 137.41, 135.82, 135.32, 135.16, 131.06, 130.27, 130.11, 127.75, 126.30, 126.14, 125.81, 123.68, 122.79, 122.03, 121.64, 118.06, 113.38, 19.85; HRMS calcd for $C_{24}H_{20}N_3O_2$ $(M+H)^+$ 382.15500, found 382.15477.

*(E)-N-(3-(3-(1H-benzo[d]imidazol-2-yl)-3-oxoprop-1-en-1-yl)phenyl)-3-methylbenzamide (**6i**).* Yellow solid; yield: 56%; m.p.: 225.4–227.2 °C; $^1$H NMR (400 MHz, DMSO) δ 10.42 (s, 1H), 8.38 (s, 1H), 8.18 (d, *J* = 16.1 Hz, 1H), 8.01 (d, *J* = 7.8 Hz, 1H), 7.94 (d, *J* = 16.1 Hz, 1H), 7.83(t, *J* = 7.4 Hz, 2H), 7.74 (dd, *J* = 5.8, 3.1 Hz, 2H), 7.55 (d, *J* = 7.4 Hz, 1H), 7.48 (t, *J* = 7.8 Hz, 1H), 7.44 (d, *J* = 6.4 Hz, 2H), 7.34 (dd, *J* = 6.0, 3.0 Hz, 2H), 2.42 (s, 3H); $^{13}$C NMR (101 MHz, DMSO) δ 181.58, 166.31, 150.31, 144.13, 140.46, 138.23, 135.18, 132.78, 129.98, 128.80, 128.64, 125.96, 125.35, 124.61, 123.27, 122.32, 119.08, 21.46; HRMS calcd for $C_{24}H_{20}N_3O_2$ $(M+H)^+$ 382.15500, found 382.15494.

*(E)-N-(3-(3-(1H-benzo[d]imidazol-2-yl)-3-oxoprop-1-en-1-yl)phenyl)-4-methylbenzamide (**6j**).* Yellow solid; yield: 52%; m.p.: 264.4–266.2 °C; $^1$H NMR (400 MHz, DMSO) δ 10.36 (s, 1H), 8.38 (s, 1H), 8.15 (d, *J* = 16.1 Hz, 1H), 8.02–7.94 (m, 4H), 7.76 (s, 2H), 7.55 (d, *J* = 7.6 Hz, 1H), 7.49 (t, *J* = 7.8 Hz, 1H), 7.38 (m, 4H), 2.40 (s, 3H); $^{13}$C NMR (101 MHz, DMSO) δ 181.19, 166.01, 149.42, 144.57, 142.28, 140.50, 135.07, 132.26, 129.98, 129.44 , 128.21, 125.98, 123.41, 121.95, 119.13, 21.50; HRMS calcd for $C_{24}H_{20}N_3O_2$ $(M+H)^+$ 382.15500, found 382.15500.

*(E)-N-(3-(3-(1H-benzo[d]imidazol-2-yl)-3-oxoprop-1-en-1-yl)phenyl)-2-(trifluoromethyl)benzamide (**6k**).* Yellow solid; yield: 51%; m.p.: 200.4–202.1 °C; $^1$H NMR (400 MHz, DMSO) δ 10.65 (s, 1H), 8.36 (d, *J* = 0.88 Hz, 2H), 8.33 (d, *J* = 8.0 Hz, 1H), 8.16 (d, *J* = 16.1 Hz, 1H), 8.01–7.96 (m, 3H), 7.83 (t, *J* = 7.8 Hz, 1H), 7.75 (s, 2H), 7.59 (d, *J* = 7.7 Hz, 1H), 7.51 (t, *J* = 7.8 Hz, 1H), 7.38 (dd, *J* = 6.1, 3.1 Hz, 2H); $^{13}$C NMR (101 MHz, DMSO) δ 181.21, 164.69, 149.44, 144.37, 140.05, 136.03, 135.17, 132.35, 130.24, 130.08, 126.39, 124.79, 124.75, 124.71, 123.56, 122.10, 119.37; HRMS calcd for $C_{24}H_{17}F_3N_3O_2$ $(M+H)^+$ 436.12674, found 436.12696.

*(E)-N-(3-(3-(1H-benzo[d]imidazol-2-yl)-3-oxoprop-1-en-1-yl)phenyl)-2-methoxybenzamide (**6l**).* Yellow solid; yield: 58%; m.p.: 225.9–227.4 °C; $^1$H NMR (400 MHz, DMSO) δ 10.29 (s, 1H), 8.33 (s, 1H), 8.11 (d, *J* = 16.1 Hz, 1H), 7.94 (d, *J* = 16.1 Hz, 1H), 7.86 (d, *J* = 8.0 Hz, 1H), 7.75 (s, 2H), 7.66 (d, *J* = 7.4 Hz, 1H), 7.56–7.44 (m, 3H), 7.36 (dd, *J* = 5.9, 2.9 Hz, 2H), 7.17 (d, *J* = 8.4 Hz, 1H), 7.07 (t, *J* = 7.4 Hz, 1H), 3.91 (s, 3H); $^{13}$C NMR (101 MHz, DMSO) δ 181.25, 165.32, 156.96, 149.42, 144.53, 140.25, 135.18, 132.61, 130.12, 130.06, 125.56, 125.26, 122.87, 122.05, 120.94, 118.91, 112.43, 56.36; HRMS calcd for $C_{24}H_{20}N_3O_3$ $(M+H)^+$ 398.14992, found 398.17975.

*(E)-N-(3-(3-(1H-benzo[d]imidazol-2-yl)-3-oxoprop-1-en-1-yl)phenyl)-4-methoxybenz amide (**6m**).* Yellow solid; yield: 63%; m.p.: 271.0–272.4 °C; $^1$H NMR (400 MHz, DMSO) δ 10.27 (s, 1H), 8.36 (s, 1H), 8.13 (d, *J* = 16.1 Hz, 1H), 8.03–7.93 (m, 4H), 7.74 (s, 2H), 7.52 (d, *J* = 7.7 Hz, 1H), 7.45 (t, *J* = 7.8 Hz, 1H), 7.37 (dd, *J* = 6.1, 3.1 Hz, 2H), 7.08 (d, *J* = 8.8 Hz, 2H), 3.84 (s, 3H); $^{13}$C NMR (101 MHz, DMSO) δ 181.20, 165.54, 162.50, 149.43, 144.58, 140.59, 135.03, 130.11, 129.94, 127.14, 125.86, 123.38, 121.90, 119.04, 114.11, 55.89; HRMS calcd for $C_{24}H_{20}N_3O_3$ $(M+H)^+$ 398.14992, found 368.14978.

*(E)-N-(3-(3-(1H-benzo[d]imidazol-2-yl)-3-oxoprop-1-en-1-yl)phenyl)-3,5-dichlorobe nzamide (**6n**).* Yellow solid; yield: 36%; m.p.: 282.4–284.6 °C; $^1$H NMR (400 MHz, DMSO) δ 10.59 (s, 1H), 8.32 (s, 1H), 8.13 (d, *J* = 16.1 Hz, 1H), 8.03 (s, 2H), 7.95 (t, *J* = 9.7 Hz, 2H), 7.87 (s, 1H), 7.74 (s, 2H), 7.58 (d, *J* = 7.5 Hz, 1H), 7.49 (t, *J* = 7.8 Hz, 1H), 7.38 (dd, *J* = 5.9, 2.9 Hz, 2H); $^{13}$C NMR (101 MHz, DMSO) δ 181.07, 163.31, 149.31, 144.38, 139.86, 138.29, 135.15, 134.82, 131.55, 130.09, 127.02, 126.47, 125.07, 123.48, 122.09, 119.34; HRMS calcd for $C_{23}H_{16}Cl_2N_3O_2$ $(M+H)^+$ 436.06141, found 436.06139.

*(E)-N-(3-(3-(1H-benzo[d]imidazol-2-yl)-3-oxoprop-1-en-1-yl)phenyl)-3,5-dimethylbe nzamide (**6o**).* Yellow solid; yield: 51%; m.p.: 220.8–222.4 °C; $^1$H NMR (400 MHz, DMSO) δ 10.38 (s, 1H), 8.37 (s, 1H), 8.16 (d, *J* = 16.0 Hz, 1H), 7.98 (t, *J* = 16.1 Hz, 2H), 7.77 (dd, *J* = 6.1, 3.2 Hz, 2H), 7.63 (s, 2H), 7.57 (d, *J* = 7.7 Hz, 1H), 7.48 (t, *J* = 7.9 Hz, 1H), 7.41 (dd, *J* = 6.2, 3.1 Hz, 2H), 7.23 (s, 1H), 2.37 (s, 6H); $^{13}$C NMR (101 MHz, DMSO) δ 180.69, 166.40, 148.94, 144.88, 140.51, 138.06, 135.15, 135.02, 133.47, 129.97, 125.88, 125.84, 125.32, 123.47, 121.91, 119.42, 21.35; HRMS calcd for $C_{25}H_{22}N_3O_2$ $(M+H)^+$ 396.17065, found 396.17045.

*General procedure for preparation of intermediates (**7a–i**)*

According to the procedure for **5a–o**, the intermediates **7a–i** were obtained from intermediate **4** with benzene sulfonyl chloride. The spectral data are summarized in the Supplementary Information.

*General procedure for preparation of target compounds (**8a–i**)*

According to the procedure for compounds **6a–i**, target compounds **8a–i** were obtained from intermediate **4** and **7a–i** in the presence of NaOH in ethanol.

*(E)-N-(3-(3-(1H-benzo[d]imidazol-2-yl)-3-oxoprop-1-en-1-yl)phenyl)-2-chlorobenzen esulfonamide (**8a**).* Yellow solid; yield: 53%; m.p.: 257.3–259.1 °C; $^1$H NMR (400 MHz, DMSO) δ 13.52 (s, 1H), 10.85 (s, 1H), 8.15 (d, *J* = 7.8 Hz, 1H), 8.00 (d, *J* = 16.1 Hz, 1H), 7.90 (d, *J* = 8.0 Hz, 1H), 7.83 (d, *J* = 16.1 Hz, 1H), 7.64 (d, *J* = 6.1 Hz, 2H), 7.61–7.55 (m, 3H), 7.49 (d, *J* = 7.7 Hz, 1H), 7.42 (t, *J* = 7.9 Hz, 1H), 7.35 (t, *J* = 7.8 Hz, 2H), 7.22 (d, *J* = 8.1 Hz, 1H); $^{13}$C NMR (101 MHz, DMSO) δ 181.15, 149.36, 143.75, 143.51, 138.35, 136.76, 135.68, 135.34, 132.44, 132.17, 131.23, 130.61,

128.33, 126.34, 125.34, 123.72, 122.57, 121.74, 121.70, 118.52, 113.38; HRMS calcd for $C_{22}H_{17}ClN_3O_3S$ $(M+H)^+$ 438.06737, found 438.06733.

*(E)-N-(3-(3-(1H-benzo[d]imidazol-2-yl)-3-oxoprop-1-en-1-yl)phenyl)-3-chlorobenzen esulfonamide (**8b**).* Yellow solid; yield: 47%; m.p.: 209.6–210.9 °C; $^1$H NMR (400 MHz, DMSO) δ 13.52 (s, 1H), 10.58 (s, 1H), 8.02 (d, *J* = 16.1 Hz, 1H), 7.87 (t, *J* = 16.0, 6.3 Hz, 2H), 7.82 (t, *J* = 1.7 Hz, 1H), 7.76 (d, *J* = 7.8 Hz, 1H), 7.74–7.71 (m, 1H), 7.62 (d, *J* = 7.9 Hz, 1H), 7.61–7.56 (m, 3H), 7.42 (m, 2H), 7.34 (t, *J* = 7.9 Hz, 1H), 7.24 (dd, *J* = 8.2, 1.2 Hz, 1H) ; $^{13}$C NMR (101 MHz, DMSO) δ 181.17, 149.34, 143.72, 143.50, 141.54, 138.49, 135.79, 135.31, 134.40, 133.61, 131.95, 130.72, 126.71, 126.35, 125.97, 125.93, 123.71, 123.19, 122.61, 121.68, 120.18, 113.38; HRMS calcd for $C_{22}H_{17}ClN_3O_3S$ $(M+H)^+$ 438.06737, found 438.06737.

*(E)-N-(3-(3-(1H-benzo[d]imidazol-2-yl)-3-oxoprop-1-en-1-yl)phenyl)-4-chlorobenzen esulfonamide (**8c**).* Yellow solid; yield: 58%; m.p.: 261.7–263.8 °C; $^1$H NMR (400 MHz, DMSO) δ 10.58 (s, 1H), 8.02 (d, *J* = 16.1 Hz, 1H), 7.88–7.83 (m, 2H), 7.81 (s, 1H), 7.74 (s, 2H), 7.65 (d, *J* = 8.6 Hz, 2H), 7.55 (d, *J* = 6.9 Hz, 2H), 7.40–7.36 (m, 3H), 7.23 (d, *J* = 7.5 Hz, 1H); $^{13}$C NMR (101 MHz, DMSO) δ 181.15, 149.34, 143.77, 138.65, 138.59, 138.46, 135.76, 130.67, 130.03, 129.13, 125.80, 123.02, 122.60, 119.97; HRMS calcd for $C_{22}H_{17}ClN_3O_3S$ $(M+H)^+$ 438.06737, found 438.06729.

*(E)-N-(3-(3-(1H-benzo[d]imidazol-2-yl)-3-oxoprop-1-en-1-yl)phenyl)-2-methylbenzen esulfonamide (**8d**).* Yellow solid; yield: 53%; m.p.: 258.4–260.0 °C; $^1$H NMR (400 MHz, DMSO) δ 13.51 (s, 1H), 10.63 (s, 1H), 8.01 (d, *J* = 8.6 Hz, 1H), 7.99 (s, 1H), 7.90 (d, *J* = 8.1 Hz, 1H), 7.82 (d, *J* = 16.1 Hz, 1H), 7.59 (d, *J* = 8.1 Hz, 1H), 7.54 (s, 1H), 7.52 (d, *J* = 15.4 Hz , 1H), 7.46 (d, *J* = 8.2 Hz , 1H), 7.41 (t, *J* = 7.5 Hz, 3H), 7.34–7.38 (m, 2H), 7.20 (d, *J* = 8.0 Hz, 1H), 2.63 (s, 3H); $^{13}$C NMR (101 MHz, DMSO) δ 181.15, 149.37, 143.82, 143.51, 138.87, 137.84, 137.31, 135.63, 135.32, 133.70, 133.19, 130.57, 129.93, 126.90, 126.34, 125.02, 123.71, 122.48, 121.68, 121.47, 118.07, 113.38, 20.21; HRMS calcd for $C_{23}H_{20}N_3O_3S$ $(M+H)^+$ 418.12199, found 418.12181.

*(E)-N-(3-(3-(1H-benzo[d]imidazol-2-yl)-3-oxoprop-1-en-1-yl)phenyl)-3-methylbenzen esulfonamide (**8e**).* Yellow solid; yield: 58%; m.p.: 244.5–256.2°C; $^1$H NMR (400 MHz, DMSO) δ 13.52 (s, 1H), 10.47 (s, 1H), 8.01 (d, *J* = 16.1 Hz, 1H), 7.87 (dd, *J* = 16.4, 8.2 Hz, 2H), 7.68 (s, 1H), 7.61 (t, *J* = 8.2 Hz, 2H), 7.56 (s, 1H), 7.51 (d, *J* = 7.7 Hz, 1H), 7.46–7.41 (m, 3H), 7.35 (t, *J* = 8.3 Hz, 2H), 7.24 (d, *J* = 8.0 Hz, 1H), 2.36 (s, 3H); $^{13}$C NMR (101 MHz, DMSO) δ 181.16, 149.36, 143.85, 143.51, 139.76, 139.57, 139.01, 135.62, 135.32, 134.19, 130.57, 129.68, 127.39, 126.33, 125.64, 124.36, 123.71, 122.74, 122.45, 121.67, 119.26, 113.38, 21.29; HRMS calcd for $C_{23}H_{20}N_3O_3S$ $(M+H)^+$ 418.12199, found 418.12192.

*(E)-N-(3-(3-(1H-benzo[d]imidazol-2-yl)-3-oxoprop-1-en-1-yl)phenyl)-4-methylbenzen esulfonamide (**8f**).* Yellow solid; yield: 40%; m.p.: 283.0–284.8°C; $^1$H NMR (400

MHz, DMSO) δ 10.42 (s, 1H), 8.00 (d, *J* = 16.1 Hz, 1H), 7.84 (d, *J* = 16.1 Hz, 1H), 7.71 (d, *J* = 8.1 Hz, 4H), 7.56 (s, 1H), 7.51 (d, *J* = 7.8 Hz, 1H), 7.35 (t, *J* = 7.6 Hz, 5H), 7.23 (d, *J* = 8.0 Hz, 1H), 2.31 (s, 3H); $^{13}$C NMR (101 MHz, DMSO) δ 181.16, 149.35, 143.93, 143.88, 139.09, 136.91, 135.62, 130.56, 130.26, 127.24, 125.50, 122.67, 122.46, 119.41, 21.44 ; HRMS calcd for $C_{23}H_{20}N_3O_3S$ $(M + H)^+$ 418.12199, found 418.12197.

*(E)-N-(3-(3-(1H-benzo[d]imidazol-2-yl)-3-oxoprop-1-en-1-yl)phenyl)-3,5-dichlorobe nzenesulfonamide (**8g**).* Yellow solid; yield: 50%; m.p.: 262.1–264.3 °C; $^1$H NMR (400 MHz, DMSO) δ 13.52 (s, 1H), 10.66 (s, 1H), 8.04 (d, *J* = 16.1 Hz, 1H), 7.94 (s, 1H), 7.88 (d, *J* = 16.0 Hz 2H), 7.77 (s, 2H), 7.63–7.57 (m, 3H), 7.42 (dd, *J* = 10.0, 5.7 Hz, 2H), 7.35 (d, *J* = 7.6 Hz, 1H), 7.25 (d, *J* = 8.1 Hz, 1H); $^{13}$C NMR (101 MHz, DMSO) δ 181.18, 149.34, 143.62, 142.70, 138.07, 135.91, 135.63, 133.32, 130.81, 126.25, 125.71, 123.52, 122.72, 120.73; HRMS calcd for $C_{22}H_{16}Cl_2N_3O_3S$ $(M+H)^+$ 472.02839, found 472.02839.

*(E)-N-(3-(3-(1H-benzo[d]imidazol-2-yl)-3-oxoprop-1-en-1-yl)phenyl)-3,5-dimethylbe nzenesulfonamide (**8h**).* Yellow solid; yield: 41%; m.p.: 258.6–259.8 °C; $^1$H NMR (400 MHz, DMSO) δ 10.40 (s, 1H), 8.00 (d, *J* = 16.1 Hz, 1H), 7.84 (d, *J* = 16.2 Hz, 2H), 7.63–7.53 (m, 4H), 7.49 (d, *J* = 7.3 Hz, 1H), 7.38–7.32 (m, 3H), 7.30 (d, *J* = 7.9 Hz, 1H), 7.24 (d, *J* = 7.6 Hz, 1H), 2.25 (s, 3H), 2.21 (s, 3H); $^{13}$C NMR (101 MHz, DMSO) δ 181.13, 149.33, 143.87, 142.76, 139.12, 138.15, 137.10, 135.55, 130.58, 130.51, 127.77, 125.47, 124.74, 122.55, 122.37, 119.04, 19.81, 19.80; HRMS calcd for $C_{24}H_{22}N_3O_3S$ $(M+H)^+$ 432.13764, found 432.13763.

*(E)-N-(3-(3-(1H-benzo[d]imidazol-2-yl)-3-oxoprop-1-en-1-yl)phenyl)-3,4-dimethylbe nzenesulfonamide (**8i**).* Yellow solid; yield: 53%; m.p.: 275.2–277.3 °C; $^1$H NMR (400 MHz, DMSO) δ 13.52 (s, 1H), 10.42 (s, 1H), 8.01 (d, *J* = 16.1 Hz, 1H), 7.86 (t, *J* = 16.2, 9.9 Hz, 2H), 7.59 (d, *J* = 8.1 Hz, 1H), 7.55 (s, 1H), 7.50 (d, *J* = 7.8 Hz, 1H), 7.47 (s, 2H), 7.42 (t, *J* = 7.2 Hz, 1H), 7.38 (d, *J* = 8.0 Hz, 1H), 7.36–7.33 (m, 1H), 7.25–7.22 (m, 2H), 2.32 (s, 6H); $^{13}$C NMR (101 MHz, DMSO) δ 181.15, 149.36, 143.89, 143.50, 139.76, 139.36, 139.06, 135.58, 135.32, 134.93, 130.57, 126.34, 125.69, 124.65, 123.72, 122.70, 122.38, 121.65, 118.90, 113.39, 21.19; HRMS calcd for $C_{24}H_{22}N_3O_3S$ $(M+H)^+$ 432.13764, found 432.13759.

### *5.3. Pharmacology*

#### *5.3.1 MTT assay in vitro*

The anti-tumor activities of compounds **6a–o** and **8a–i** were evaluated against HCT116, MCF7 and 143B cell lines *in vitro* using a standard MTT assay, with odanacatib and 5-FU as the positive controls. Compounds were tested at six concentrations (0.001–100 μM).

The tumor cell lines were cultured in RPMI 1640 medium (Sigma, Germany), supplemented with 10% fetal bovine serum (FBS, Sigma). Approximately $4\times10^3$ cells,

suspended in RPMI 1640 medium, were plated into each well of a 96-well plate and incubated at 37°C for 24 h in 5% $CO_2$. The test compounds were then added to the culture medium and the cells were incubated for a further 48 h. Fresh MTT was added to each well at the terminal concentration (0.5 mg/mL) and the cells were incubated at 37°C for 4 h in 5% $CO_2$. DMSO (150 μL) was then added to each well to dissolve the formazan crystals and the absorbance was measured at 540 nm using a microplate reader (HEALES MB-580, China). The results, expressed as $IC_{50}$ values, were the average of three determinations and were calculated using SPSS software.

*5.3.2 Molecular docking*

The X-ray crystal structure of Cat K (PDB code 1NLJ) was used for the docking studies. 1NLJ was processed using the Protein Preparation protocol of Sybyl-X2.0. Firstly, the ligand was extracted from the complex to determine the location of the active site. Secondly, backbones and sidechains of the protein were repaired. Thirdly, all hydrogen atoms were added and the protein was protonated at pH 7.4. Fourthly, an Amber7 FF99 force field was applied to the biopolymer. A Surflex-Dock Control File containing information about the protein and the active site was then defined with a threshold value of 0.5. The maximum number of poses per ligand was set to 10. The ligand in the crystal structure was defined as the reference molecule. Finally, structure-based docking was carried out using the Surflex-Dock Geom mode of Sybyl-X2.0.

The docking studies for compound **8e** with other cysteine cathepsins (CatB, CatL, CatS, CatF, CatH, CatV and CatX) were performed using the same method as for Cat K.

*5.3.3 In vitro enzymatic assays*

The Cat K inhibitory activity of the compounds was determined using a previously described method,[43] with minor modifications. Compounds were screened at 5 μM to evaluate the enzymatic inhibition.

Recombinant human Cat K (5.5 ng/mL) in reaction buffer (50 μL) containing sodium acetate (50 mM), EDTA (2.5 mM) and DTT (1 mM) was added to a 96-well plate containing the test compounds at pH 6.0. The plate was incubated at 37°C for 15 min and the reaction was then initiated by adding a solution of the substrate, Z-Phe-Arg-AMC (20 μL, 10 μM). After 30 min, the fluorescence intensity was measured (excitation at 355 nm; emission at 460 nm) using a microplate reader (Wallac 1420 Victor2, Perkin-Elmer, USA). The inhibition rate was determined using the fluorescence intensity.

The Cat L, Cat S and Cat B inhibitory assays were carried out using a similar procedure to Cat K, except that the Cat S and Cat B substrates were replaced with Ac-Lys-Gln-Lys-Leu-Arg-AM.C and Z-Arg-Arg-AMC, respectively.

## Acknowledgements

The work was supported by the National Natural Science Foundation of China (81473097), Student Fund of Innovation Project of Peking Union Medical College

(2015-1007-22), and the CAMS initiative for Innovative Medicine (2016-I2M-3-022).

## Supporting information

The interactions between 6i and enzymes (Cat K and Cat L) were presented in Figure S1. The enzyme activity of the compound without benzenesulfonamide or benzamide group was listed in Table S1. The spectral data of intermidiates **5a–o** and **7a–i** are summarized, followed by the $^{1}H$ NMR spectrum, $^{13}C$ NMR spectrum and high resolution mass spectrum of target compounds **6a–o** and **8a–i**.

## References

1. Vasiljeva O, Turk B. *Biochimie*. 2008; 90: 380-386.
2. Gocheva V, Joyce JA. *Cell Cycle*. 2007; 6: 60-64.
3. Jedeszko C, Sloane BF. *Biol Chem*. 2004; 385: 1017-1027.
4. Joyce JA, Hanahan D. *Cell Cycle*. 2004; 3: 1516-1519.
5. Mohamed MM, Sloane BF. *Nat Rev Cancer*. 2006; 6: 764-775.
6. Yasuda Y, Kaleta J, Bromme D. *Adv Drug Deliv Rev*. 2005; 57: 973-993.
7. Pozgan U, Caglic D, Rozman B, et al. *Biol Chem*. 2010; 391: 571-579.
8. Cheng XW, Huang Z, Kuzuya M, et al. *Hypertension*. 2011; 58: 978-986.
9. Kos J, Lah TT. *Oncology Reports*. 1998; 5: 1349-1361.
10. dos Santos DA, Deobald AM, Cornelio VE, et al. *Bioorg Med Chem*. 2017; 25: 4620-4627.
11. Tamhane T, Lllukkumbura R, Lu S, et al. *Biochimie*. 2016; 122: 208-218.
12. Lah TT, Kos J, Blejec A, et al. *Pathol Oncol Res*. 1997; 3: 89-99.
13. Chen Q, Fei J, Wu L, et al. *Oncol Lett*. 2011; 2: 693-699.
14. Frohlich E, Schlagenhauff B, Mohrle M, et al. *Cancer*. 2001; 91: 972-982.
15. Singh N, Das P, Datta Gupta S, et al. *Cancer Invest*. 2013; 31: 461-471.
16. Quintanilla-Dieck MJ, Codriansky K, Keady M, et al. *J Invest Dermatol*. 2008; 128: 2281-2288.
17. Herroon MK, Rajagurubandara E, Rudy DL, et al. *Oncogene*. 2013; 32: 1580-1593.
18. Lindeman JHN, Hanemaaijer R, Mulder A, et al. *The American Journal of Pathology*. 2004; 165: 593-600.
19. Ishida M, Kojima F, Okabe H. *J Eur Acad Dermatol Venereol*. 2013; 27: 128-130.
20. Littlewood-Evans AJ, Bilbe G, Bowler WB, et al. *Cancer Research*. 1997; 57: 5386-5390.
21. Husmann K, Muff R, Bolander ME, et al. *Mol Carcinog*. 2008; 47: 66-73.
22. Jensen AB, Wynne C, Ramirez G, et al. *Clin Breast Cancer*. 2010; 10: 452-458.
23. Schurigt U, Sevenich L, Vannier C, et al. *Biol Chem*. 2008; 389: 1067-1074.
24. Le Gall C, Bellahcene A, Bonnelye E, et al. *Cancer Research*. 2007; 67: 9894-9902.
25. Raghav N, Singh M. *Eur J Pharm Sci*. 2014; 54: 28-39.
26. Kim SH, Lee E, Baek KH, et al. *Bioorg Med Chem Lett*. 2013; 23: 3320-3324.
27. Garg S, Raghav N. *RSC Adv*. 2015; 5: 72937-72949.
28. Ramalho SD, Bernades A, Demetrius G, et al. *Chem Biodivers*. 2013; 10:

1999-2006.
29. Raghav N, Singh M. *Bioorg Med Chem.* 2014; 22: 4233-4245.
30. Raghav N, Kaur R. *Int J Biol Macromol.* 2015; 80: 710-724.
31. Parker EN, Song J, Kishore Kumar GD, et al. *Bioorg Med Chem.* 2015; 23: 6974-6992.
32. Sahu NK, Balbhadra SS, Choudhary J, et al. *Curr Med Chem.* 2012; 19: 209-225.
33. Deb Majumdar I, Devanabanda A, Fox B, et al. *Biochem Biophys Res Commun.* 2011; 416: 397-402.
34. Gauthier JY, Chauret N, Cromlish W, et al. *Bioorg Med Chem Lett.* 2008; 18: 923-928.
35. Ahmad S, Siddiqi MI. *J Mol Model.* 2017; 23: 92-108.
36. Yamamoto A, Tomoo K, Hara T, et al. *J Biochem.* 2000; 127: 635-643.
37. Szcześniak P, Pieczykolan M，Stecko S. *J Org Chem.* 2016; 81: 1057-1074.
38. Schroder J, Klinger A, Oellien F, et al. *J Med Chem.* 2013; 56: 1478-1490.
39. Wu LT, Jiang Z, Shen JJ, et al. *Eur J Med Chem.* 2016; 114: 328-336.
40. Reddy VM, REddy KR. *Chem Pharm Bull.* 2010; 58: 953-956.
41. Vazquez ME, Blanco JB, Imperiali B. *J Am Chem Soc.* 2005; 127: 1300-1306.
42. Cai X, Qian CG, Zhai HX, US 20140018368A1.
43. Bromme D, Steinert A, Friebe S, et al. *Biochem J.* 1989; 264: 475-481.

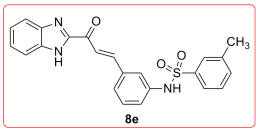


8e

**Cell activity**

HCT116 $IC_{50}$ = 0.597 μM
MCF7 $IC_{50}$ = 0.886 μM
143B $IC_{50}$ = 0.791 μM

**Enzyme inhibitory rate**

Cat L 92.35%
Cat K 93.46%